Journal of Hazardous Materials 161 (2009) 737–746

Contents lists available at ScienceDirect

Journal of Hazardous Materials

journal homepage: www.elsevier.com/locate/jhazmat

Removal of copper(II) from aqueous phase by Purolite C100-MB cation exchange resin in fixed bed columns: Modeling

Oualid Hamdaoui*

Department of Process Engineering, Faculty of Engineering, University of Annaba, P.O. Box 12, 23000 Annaba, Algeria

ARTICLE INFO

Article history:
Received 25 November 2007
Received in revised form 6 April 2008
Accepted 7 April 2008
Available online 11 April 2008

Keywords:
Water treatment
Copper
Fixed bed
Ion exchange resin
Modeling

ABSTRACT

The dynamic removal of copper by Purolite C100-MB cation exchange resin was studied in packed bed columns. The values of column parameters are predicted as a function of flow rate and bed height. Batch experiments were performed using the Na-form resin to determine equilibrium and kinetics of copper removal. The uptake of Cu(II) by this resin follows first-order kinetics. The effect of stirring speed and temperature on the removal kinetics was studied. The activation energy for the exchange reaction is 13.58 kJ mol^{-1}. The equilibrium data obtained in this study have been found to fit both the Langmuir and Freundlich isotherm equations. A series of column tests were performed to determine the breakthrough curves with varying bed heights and flow rates. To predict the breakthrough curves and to determine the characteristic parameters of the column useful for process design, four kinetic models; Bohart–Adams, Bed Depth Service Time (BDST), Clark and Wolborska models are applied to experimental data. All models are found suitable for describing the whole or a definite part of the dynamic behavior of the column with respect to flow rate and bed height. The simulation of the whole breakthrough curve is effective with the Bohart–Adams and the Clark models, but the Bohart–Adams model is better. The breakthrough is best predicted by the Wolborska model. The breakthrough data gave a good fit to the BDST model, resulting in a bed exchange capacity very close to the value determined in the batch process.

1. Introduction

Modern society is increasingly concerned by environmental issues related to industrial activity and polluting industries have to conform to a more and more rigid environmental regulation. Basic metals such as aluminum, cadmium, chromium, copper, iron, lead, mercury, nickel, and zinc have been classified as the metals of primary importance for recovery from industrial waste streams [1]. Metal ions contained in wastewater have to be recovered using conventional methods based on precipitation, electrochemistry, solvent extraction or ion exchange resins.

The production of ion exchange resins is a technology that relies on the chemical interaction between reactive entities to form stable covalent bonds between a water insoluble support and a water-soluble functional group possessing a positive or negative charge.

Ion exchange is a unit operation in its own right, often sharing theory with adsorption, although it has its own special areas of application. Ion exchange using polymeric resins has been used successfully to recover heavy metals from wastewaters and process streams [2–6]. Many studies on the removal of metal ions by ion exchange resins have been conducted [2,7–18]. It has been reported that ion exchange is able to overcome some of the problems encountered in other techniques.

Knowledge of exchange phenomena at the solid–liquid interface is also crucial for understanding the fate and transport of environmental contaminants, which commonly come into contact with surfaces that provide sites with which ions interact. For a comprehensive representation of such phenomena, it is necessary to account for ion exchange as well as chemical equilibria.

The aim of the present work is to study and model the removal of copper from aqueous solutions by Purolite C100-MB ion exchange resin in fixed bed columns. This resin is not selective for copper that is used as a model of metal ions. Other bivalent ions and many heavy metals present in industrial effluents will be competitors of copper. Thus, the possible competition effects are not taken into account in this work. The effects of flow rate and bed height are explored during the column test. Additionally, equilibrium and kinetic parameters of Cu(II) removal by the Purolite C100-MB resin was studied in a batch mode. The influence of agitation speed and temperature on the copper uptake kinetics by the ion exchange resin was investigated.

* Tel.: +213 771 598 509; fax: +213 38 87 65 60.
E-mail address: ohamdaoui@yahoo.fr.

0304-3894/$ – see front matter © 2008 Elsevier B.V. All rights reserved.
doi:10.1016/j.jhazmat.2008.04.016

Nomenclature

A	constant in the Clark model
A_0	is the temperature independent factor in the Arrhenius equation ($L\,g^{-1}\,min^{-1}$)
b	Langmuir constant ($L\,mg^{-1}$)
B	internal diffusion rate constant (min^{-1})
C	effluent metal ions concentration ($mg\,L^{-1}$)
C_e	equilibrium concentration of metal ions in the aqueous phase ($mg\,L^{-1}$)
C_0	inlet (feed) or initial concentration of metal ions in the aqueous phase ($mg\,L^{-1}$)
[Cu(II)]	liquid-phase concentration of copper ($mg\,L^{-1}$)
D	axial diffusion coefficient ($mm^2\,h^{-1}$)
D_i	the effective diffusion coefficient of the metal ions in the resin phase ($m^2\,min^{-1}$)
E_a	activation energy of reaction ($kJ\,mol^{-1}$)
K_{app}	apparent rate constant (min) or apparent rate constant by unit weight of resin ($L\,g^{-1}\,min^{-1}$)
K_{BA}	kinetic constant in the Bohart–Adams model ($L\,mg^{-1}\,h^{-1}$)
K_C	mass-transfer coefficient in the Clark model (h^{-1})
K_F	Freundlich constant ($mg^{1-(1/n)}\,L^{1/n}\,g^{-1}$)
m	an integer that defines the infinite series solution
n	Freundlich constant
n_0	maximum amount of metal exchanged in the dynamic process ($mg\,g^{-1}$)
N_0	maximum amount of metal exchanged in the dynamic process ($mg\,L^{-1}$)
q	amount of metal exchanged at any time t ($mg\,g^{-1}$)
q_e	amount of metal exchanged at equilibrium ($mg\,g^{-1}$)
q_m	maximum amount of metal exchanged ($mg\,g^{-1}$)
Q	flow rate ($mL\,h^{-1}$)
r	constant in the Clark model (h^{-1})
r_0	the radius of the sorbent particle (m)
R	coefficient of correlation
R_g	universal gas constant ($8.314\,J\,mol^{-1}\,K^{-1}$)
R_L	dimensionless equilibrium parameter of Hall
t	time (h)
t_b	time at breakthrough (h)
T	solution temperature (K)
U_0	superficial velocity ($mm\,h^{-1}$)
v	migration rate ($mm\,h^{-1}$)
V	volume of solution (L)
W	weight of dry resin (g)
Z	height of the bed (mm)
Z_0	thickness of mass-transfer zone (mm)

Greek letter

β_a	kinetic coefficient of the external mass transfer in the Wolborska model (h^{-1})

2. Materials and methods

2.1. Resin and solutions

The strong-acid Purolite C100-MB resin with sulfonic acid $-SO_3Na$ group was supplied by the water treatment plant of the iron and steel industry complex of El Hadjar (Annaba, Algeria). The physical properties and specifications reported by the supplier are shown in Table 1. This cation exchange resin is generally used for water softening. The exchange capacity was 2.5 meq g^{-1} and its particle size was 0.42–1.2 mm. Prior to use, the resin was washed with deionized water (Millipore Milli-Q) several times and then dried in a vacuum oven at 50 °C overnight.

$CuSO_4{\cdot}5H_2O$ (from Merck, analytical grade) and UHQ water was used to prepare Cu(II) solutions.

Table 1
Characteristics of the Purolite C100-MB cation exchange resin

Characteristics	Values
Grade	Industrial grade
Physical form	Uniform particle size spherical beads
Bulk density	800 g L^{-1}
Harmonic mean size	0.55 mm
Uniformity coefficient	1.5 maximum
Particle size	0.42–1.2 mm
Functional group	$-SO_3^-$
Matrix	Polystyrene DVB gel
Ionic form	Na^+
Total exchange capacity	2.0 eq L^{-1}
Moisture	44–48%
pH range	0–14
Maximum operating temperature	120 °C

2.2. Exchange kinetics

Batch kinetic tests were conducted in the reactor shown in Fig. 1. Kinetic tests were performed in baffled 1 L glass reactor that was attached to an overhead mechanical stirrer. The reactor was immersed in a water bath at a constant temperature of 25 °C. The reaction mixture consisted of a total volume 400 mL of solution containing 0.4 g of resin. The initial copper concentration was varied from 150 to 250 mg L^{-1}. At fixed time intervals a sample of solution was withdrawn and analyzed by atomic absorption spectroscopy (PerkinElmer A310). Each experiment was performed in duplicate and the mean values were presented.

2.3. Equilibrium

For measuring the equilibrium distribution of ions between resin and liquid phases, accurately weighted amount (0.5–3 g) of ion exchange resin were continuously stirred at 250 rpm with 400 mL of 200 mg L^{-1} copper(II) aqueous solution in thermostated bath. The experiments were performed at the pH that resulted from solving the metal in water (around 5) without further adjustment. The temperature was controlled at 25 °C. Agitation was provided for 2 h, which is more than sufficient time to reach equilibrium. The contact time was determined by preliminary kinetic tests using the same conditions. After agitation, aqueous samples were taken and the concentrations of copper were analyzed by atomic absorption spectroscopy (PerkinElmer A310). The amount of metal exchanged

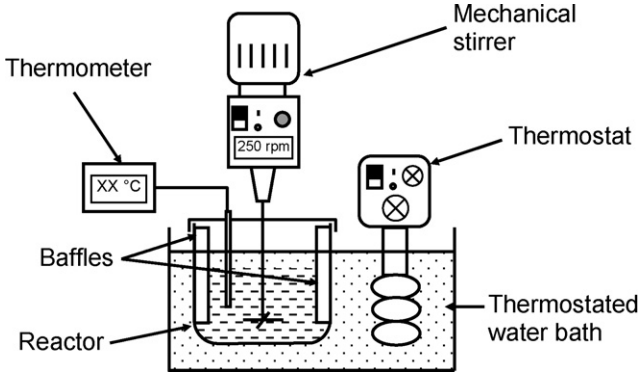

Fig. 1. Scheme of the experimental setup.

at equilibrium, q_e (mg g^{-1}), was thus calculated by

$$q_e = \frac{(C_0 - C_e)V}{W} \quad (1)$$

where C_0 and C_e are the initial and equilibrium concentrations of metal ions in the aqueous phase, respectively (mg L^{-1}), V is the solution volume (L), and W is the weight of dry resin (g).

Each experiment was performed twice at least and the mean values were presented.

2.4. Fixed bed experiments

The fixed bed experiments were carried out in a water-jacketed glass column with an inner diameter of 8 mm at a constant temperature of 25 °C. The column was packed with different bed heights (8, 12, and 16 mm) of resin on a glass-wool support and was loaded with 200 mg L^{-1} of Cu(II) solution. The experiments were performed at the pH that resulted from solving the metal in water (around 5) without further adjustment. Fixed bed up-flow exchangers were fed by a peristaltic pump at a constant flow rate, ranging from 39 to 106 mL h^{-1}. The samples in the outlet were taken at the preset time intervals and their concentrations were analyzed, as described above, to yield output concentration breakthrough curves.

In the present study, because the ratio of internal column diameter to resin particle diameter is higher than 10 (approximately 14.5), the effects of near-wall disturbances and preferential channels in the column can be neglected [19].

3. Theoretical background

Fixed bed ion exchangers share a common theory with fixed bed adsorbers. Successful design of a column exchange process requires prediction of the concentration–time profile or breakthrough curve and exchange capacity for the effluent under given specific operating conditions. Developing a model to accurately describe the dynamic behavior of exchange in a fixed bed system is inherently difficult as in such systems the concentration profiles in the liquid and solid phases vary in both space and time. Some solutions for very limiting cases have been reported, but in general, complete time-dependent analytical solutions to differential equation based models of the proposed rate mechanisms are not available. If the goal is to model the breakthrough behavior of an exchange column with a high degree of accuracy, the use of simpler and more tractable models that avoid the need for numerical solution appears more suitable and logical and could have immediate practical benefits. Because of this, various simple mathematical models have been developed to predict the dynamic behavior of the column and the following models characterizing fixed bed performance are discussed in detail here.

The breakthrough time or breakthrough point (the time at which copper concentration in the effluent reached 1 mg L^{-1}) and bed exhaustion or saturation time (the time at which copper concentration in the effluent reached influent concentration) were used to evaluate the breakthrough curves.

3.1. Bohart–Adams model

Bohart and Adams [20] established the fundamental equations describing the relationship between C/C_0 and t for the adsorption of chlorine on charcoal in fixed bed column. Although the original work by Bohart and Adams was done for the gas–charcoal adsorption system, its overall approach can be applied successfully in quantitative description of other systems. This model assumes that the adsorption rate is proportional to both the residual capacity of the activated carbon and the concentration of the sorbing species. The Bohart and Adams model is given by the following equation:

$$\ln\left(\frac{C_0}{C} - 1\right) = \frac{K_{BA}N_0Z}{U_0} - K_{BA}C_0t \quad (2)$$

where C is the effluent concentration (mg L^{-1}), C_0 is the influent concentration (mg L^{-1}), K_{BA} is the rate coefficient (L mg^{-1} h^{-1}), N_0 is the exchange capacity (mg L^{-1}), Z is the bed height (mm), U_0 is the linear velocity (mm h^{-1}), and t is the time (h).

The model constants K_{BA} and N_0 can be determined from a plot of $\ln[(C/C_0) - 1]$ against t at given flow rate and bed height.

3.2. Bed depth service time (BDST) model

The bed depth service time (BDST) relation developed by Hutchins [21] and currently used is given by:

$$t_b = \frac{N_0}{C_0U_0}(Z - Z_0) \quad (3)$$

where t_b is the breakthrough time (h), N_0 is the exchange capacity (mg L^{-1}), C_0 is the initial concentration (mg L^{-1}), U_0 is the superficial fluid velocity (mm h^{-1}), Z is the height of the fixed bed (mm), and Z_0 is the length of the dynamic bed mass-transfer zone (mm), which is equivalent to the adsorption front where sorbent material is partly saturate. This latter parameter corresponds to the critical bed depth, defined as the theoretical minimum depth of the resin sufficient to prevent an untimely release of pollutant in the effluent solution.

3.3. Clark model

The model developed by Clark [22] is based on the use of a mass-transfer concept in combination with the Freundlich isotherm:

$$\left(\frac{C_0}{C}\right)^{n-1} - 1 = A\,e^{-rt} \quad (4)$$

where n is the Freundlich parameter and A and r are the Clark constants.

$$A = \exp\left(\frac{K_CN_0Z}{U}\right) \quad (5)$$

and

$$r = K_CC_0 \quad (6)$$

linearizing Eq. (4):

$$\ln\left[\left(\frac{C_0}{C}\right)^{n-1} - 1\right] = \ln A - rt \quad (7)$$

From a plot of $\ln[(C_0/C)^{n-1} - 1]$ versus time, the values of r (h^{-1}) and A can be thus determined from its slope and intercept, respectively.

3.4. Wolborska model

Wolborska [23] has proposed a model based on the general equations of mass transfer for diffusion mechanisms in the range of the low-concentration breakthrough curve. The Wolborska model is given by the following equation:

$$\ln\frac{C}{C_0} = \frac{\beta_aC_0}{N_0}t - \frac{\beta_aZ}{U_0} \quad (8)$$

with

$$\beta_a = \frac{U_0^2}{2D}\left(\sqrt{1 + \frac{4\beta_0D}{U_0^2}} - 1\right) \quad (9)$$

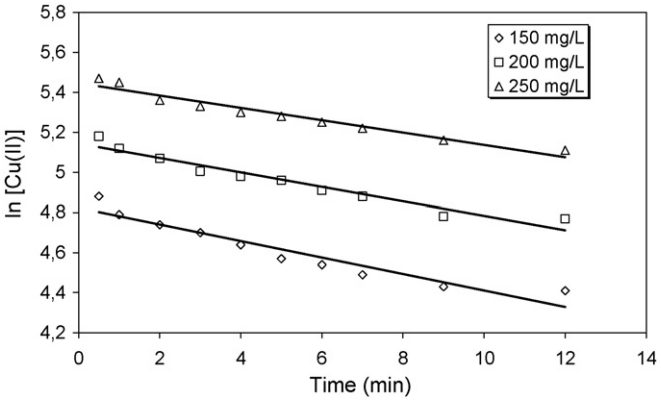

Fig. 2. Evolution of ln[Cu(II)] versus time.

where β_a is the kinetic coefficient of the external mass transfer (h^{-1}), D is the axial diffusion coefficient ($mm^2\,h^{-1}$), and β_0 is the external mass-transfer coefficient with a negligible axial dispersion coefficient D, N_0 is the exchange capacity ($mg\,L^{-1}$), U_0 is the superficial fluid velocity ($mm\,h^{-1}$) and Z is the height of the fixed bed (mm).

Wolbraska observed that in short beds or at high flow rates of solution through the bed, the axial diffusion is negligible and $\beta_a = \beta_0$. The migration velocity ($mm\,h^{-1}$) of the steady-state front satisfies the relation, known as Wicke's law:

$$v = \frac{U_0 C_0}{N_0 + C_0} \tag{10}$$

The plot of $\ln C/C_0$ versus t would give information on this model.

4. Results and discussion

4.1. Exchange kinetics

The design of most equipment requires data on the amount of ions exchanged between resin and liquid that will have occurred in a given contact time. The exchange kinetics describes the solute uptake rate which in turn governs the residence time of an exchange reaction. It is one of the important characteristics in defining the efficiency of an exchange process. Hence, in the present study, the kinetics of copper removal has been carried out to understand the behavior of the resin.

Determination of the apparent reaction order was carried out with Cu(II) initial concentrations of 150, 200, and 250 $mg\,L^{-1}$, stirring speed of 250 rpm, and constant temperature of 25 °C.

The rate for a first-order reaction for a constant volume batch system can be expressed as:

$$(-r_{app}) = -\frac{d[Cu(II)]}{dt} = K_{app}[Cu(II)] \tag{11}$$

where $(-r_{app})$ is the reaction rate ($mol\,L^{-1}\,min^{-1}$), [Cu(II)] is the liquid-phase concentration of copper ($mg\,L^{-1}$), t is the time (min), and K_{app} is the rate constant (min^{-1}).

A plot of ln[Cu(II)] versus t gives a straight line. The slope of the lines is the rate constant as represented in Fig. 2. According to Fig. 2, the rate constant for the removal of copper by the cation exchange resin is well of first-order. Moreover, the apparent rate constant show a steady decrease with an increase of the initial concentration of Cu(II) in the solution (Table 2). An increase in initial copper concentration leads to an increase of the amount of copper exchanged at equilibrium. This is a result of the increase in the driving force the concentration gradient, as an increase in the initial copper ion concentrations.

Table 2
Values of copper ion-exchange kinetic parameters for various initial concentrations: apparent rate constant (K_{app}), external diffusion rate (dq/dt), effective diffusion coefficients (D_i), and internal diffusion rate constant (B)

	C_0 ($mg\,L^{-1}$)		
	150	200	250
Apparent rate constant, $K_{app} \times 10^4$ (min^{-1})	270.24	230.29	208.50
External diffusion, dq/dt ($mg\,g^{-1}\,min^{-1}$)	22.66	20.70	19.40
Internal diffusion, $D_i \times 10^{11}$ ($m^2\,min^{-1}$)	1.50	1.68	1.96
Internal diffusion, $B \times 10^4$ (min^{-1})	4.89	5.48	6.39

Using the kinetic data, it is possible to design the characteristics of a fixed bed exchanger.

The kinetic studies help in predicting the progress of exchange, but the determination of the exchange mechanism is also important for design purposes. In ion exchange process, the transfer of ions is controlled by either boundary layer diffusion (external mass transfer), intraparticle diffusion (mass transfer through the pores) or by the exchange reaction, or by combination. In ion exchange systems, the following phenomena are involved, relevant for the process kinetics:

- diffusion of metal ions from the bulk of the solution to a liquid thin layer that surrounds each particle;
- diffusion of metal ions through this layer surrounding each resin particle to the resin surface (liquid-film diffusion);
- intraparticle diffusion of metal ions through resin channels (diffusion within the particle);
- cationic exchange (rate of reaction).

The main kinetic parameters associated with external and internal diffusions were calculated. The values of the external diffusion rate (dq/dt) of the entering ions into the resin exchanger were determined from kinetic curves [24,25]. These values shown in Table 2 were evaluated as the slope of the linear portion of this q (amount of metal exchanged, $mg\,g^{-1}$) versus t curve at short times, namely $t \to 0$. The values of the external diffusion rate remain nearly constant in the studied concentration range (150–250 $mg\,L^{-1}$). The average external diffusion rate (dq/dt) value was estimated to be 20.92 $mg\,g^{-1}\,min^{-1}$.

The kinetic parameters – diffusion rate constant (B) and diffusion coefficient (D_i) – related to the internal diffusion were determined from normalized kinetic curves. The normalized kinetic curves (figure not shown) represent the ratio of the amount of copper retained per gram of resin (q) at time t divided by the amount of copper retained per gram of resin at equilibrium (q_e) as function of the time t.

Assuming that the rate-limiting step of the ion exchange is internal diffusion, q/q_e is defined by the following equation:

$$\frac{q}{q_e} = 1 - \frac{6}{\pi^2}\sum_{m=1}^{\infty}\frac{1}{m^2}\exp\left[\frac{-D_i\pi^2 m^2 t}{r_0^2}\right] \tag{12}$$

where D_i is the effective diffusion coefficient of the metal ions in the resin phase ($m^2\,min^{-1}$), r_0 is the radius of the sorbent particle (m), assumed to be spherical, t is the time (min), and m is an integer that defines the infinite series solution.

In the normalized kinetic curves, the area (I_0) between the curves and their asymptotes is given by [24]

$$I_0 = \int_0^{\infty}\left(1 - \frac{q}{q_e}\right)dt = \frac{D_i}{15r_0^2} \tag{13}$$

The expression (13) was used to calculate the D_i values, which are shown in Table 2.

Values of the internal diffusion rate constant (B) were determined using Eq. (14). These values are provided in Table 2:

$$B = \frac{\pi^2 D_i}{r_0^2} \quad (14)$$

It can be observed that both the values of the kinetic parameters (Table 2) and the amount of copper exchanged increased with the initial concentration, which indicates that ion exchange is favored. It is also observed that an increase in the initial copper concentration increases the pore diffusion rate parameters. This is due to the increase in the bulk liquid metal concentration which increases the driving force for metal diffusion. This suggests that beside the ion exchange, other processes take place that affect the internal diffusion of the ions [24].

In many practical cases, mass transfer is controlled by a combination of resistances and consequently each step needs to be considered. In order to interpret the experimental data, it is necessary to identify the limiting step that controls the removal kinetics, among reaction rate, intraparticle diffusion or external diffusion. The detail is described later.

4.2. Effect of agitation speed

In all the experiments in which the effect of agitation speed was studied, the initial copper concentration and solution temperature were 200 mg L^{-1} and 25 °C, respectively. The agitation speed was varied from 60 to 250 rpm.

Knowing the reaction order, the rate constant is determined for each agitation speed. The evolution of the apparent rate constant, K_{app}, according to the stirring speed, shown in Fig. 3, shows the existence of two lines of different slopes with an intersection for an agitation speed of 110 rpm. This figure highlights the existence of two limiting steps. When the stirring speed is higher than 110 rpm, the apparent rate constant is independent of stirring speed. The process is controlled by intraparticle diffusion or chemical rate. The rate-limiting step for a temperature of 25 °C is the reaction rate (cf. effect of temperature). Consequently, because no change in slope is observed, it is possible to determine the true rate constant (230.35×10^{-4} min^{-1}) as well as the rate constant per unit weight of resin (230.35×10^{-4} L g^{-1} min^{-1}). When the stirring speed is lower than 110 rpm, the apparent rate constant varies according to the stirring velocity, and is lower than the true rate constant. The liquid-film external diffusion is the limiting step and controls the exchange process.

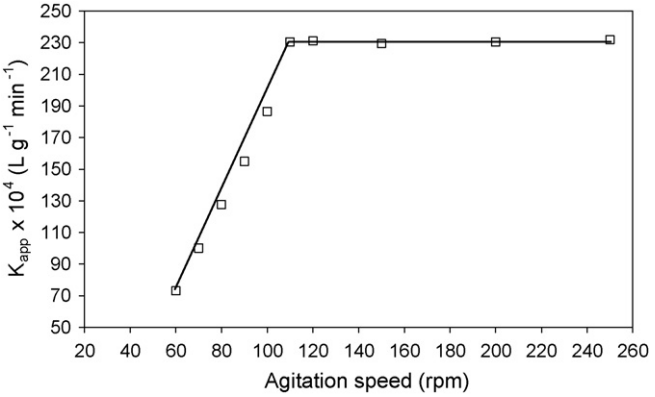

Fig. 3. Variation of the apparent rate constant versus agitation speed.

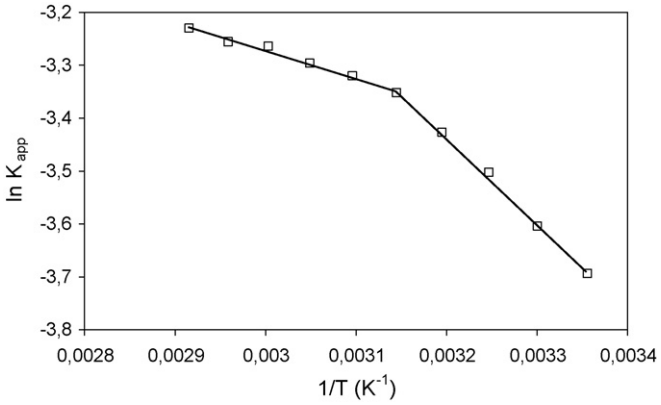

Fig. 4. Plot of ln K_{app} verus $1/T$.

4.3. Effect of temperature

To study the influence of temperature on the removal kinetics of copper by the cation exchange resin, experiments were carried out at 200 mg L^{-1} initial copper concentration and constant agitation speed of 250 rpm. The stirring speed was fixed at 250 rpm in order to overcome the external mass transfer resistance. The only possible limiting kinetic steps are the kinetic rate and particle diffusion. Experiments were carried out at various temperatures (25–70 °C).

The obtained results show that the apparent rate constant depends on temperature. From Fig. 4, it is possible to observe that the plot of ln $K_{app} = f(1/T)$ shows two linear regions. The initial linear portion obtained at low temperatures ($T < 45$ °C) corresponds to the kinetic mode. Therefore, it is possible to determine the activation energy for the exchange reaction according to Arrhenius equation:

$$K_{app} = A_0 \exp\left(-\frac{E_a}{R_g T}\right) \quad (15)$$

where A_0 is the temperature independent factor (L g^{-1} min^{-1}); E_a the reaction activation energy (kJ mol^{-1}); R_g the universal gas constant (8.314 J mol^{-1} K^{-1}); T is the solution temperature (K). From this equation, Arrhenius constant, A_0, is 5.98 L g^{-1} min^{-1} and the activation energy for exchange reaction, E_a, is 13.58 kJ mol^{-1}.

The linear portion obtained for high temperatures (>45 °C) is attributed to the transport phenomena inside solid particles. The slope of this portion (−521.46) is lower than the slope of the kinetic mode. This indicates that the rise in temperature results in a significant increase in the exchange reaction compared to the particle diffusion.

4.4. Equilibrium

If ion exchange resin is thought as a charged adsorbent, the adsorption isotherm equations can be thus applicable. The equilibrium removal of the copper ions investigated can be mathematically expressed in terms of the sorption isotherms. The exchange data are commonly fitted to the Langmuir or Freundlich models.

The Langmuir equation was applied to the exchange equilibria for the cation exchange resin (Fig. 5):

$$\frac{1}{q_e} = \frac{1}{q_m} + \frac{1}{q_m b C_e} \quad (16)$$

where C_e is the aqueous-phase metal concentration at equilibrium (mg L^{-1}), q_e is the amount of metal exchanged at equilibrium (mg g^{-1}), q_m is the maximum amount of metal exchanged (mg g^{-1}), and b is the Langmuir constant (L mg^{-1}).

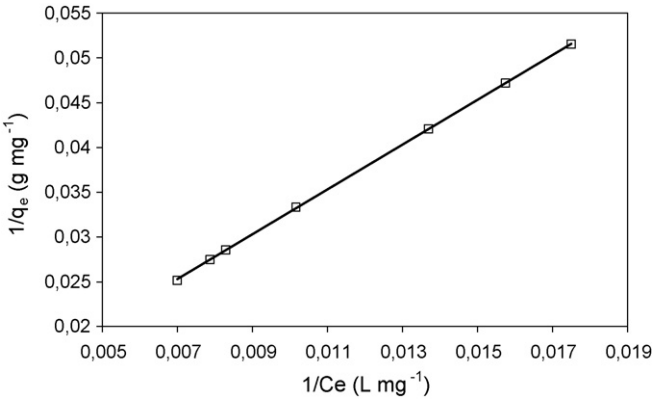

Fig. 5. Langmuir plot for copper removal by the ion exchange resin.

The equilibrium data can be modeled using the Freundlich model given by the equation (Fig. 6):

$$\ln q_e = \ln K_F + \frac{1}{n}\ln C_e \quad (17)$$

where C_e is the liquid-phase metal concentration at equilibrium ($mg\,L^{-1}$), q_e is the amount of metal exchanged at equilibrium ($mg\,g^{-1}$), and K_F ($mg^{1-(1/n)}\,L^{1/n}\,g^{-1}$) and n are the Freundlich constants.

The values of Freundlich and Langmuir parameters are presented in Table 3. The correlation coefficients indicate that both Langmuir and Freundlich equations describe well the equilibrium data. In this work, the maximum amount of metal exchanged at 25 °C is found to be 121.5 $mg\,g^{-1}$. Exchange capacity of Purolite C100-MB was compared to those of different types of resins used for removal of copper [5,11,26,27]. The value of exchange capacity in this study is larger than those in most of previous works. This suggests that copper could be easily exchanged using Purolite C100-MB resin.

In order to predict the exchange efficiency of the process, the dimensionless equilibrium parameter of Hall is determined by using the following equation [28]:

$$R_L = \frac{1}{1 + bC_0} \quad (18)$$

where C_0 is the initial metal ions concentration. Values of $R_L < 1$ represent favorable exchange. The obtained R_L-value (Table 3) shows that the studied system is favorable.

The magnitude of the exponent n gives an indication on the favorability of exchange. It is generally stated that a value of n higher than unity represent favorable exchange characteristics [29]. Table 3 indicates that n is greater than unity, indicating that copper is favorably exchanged by the resin.

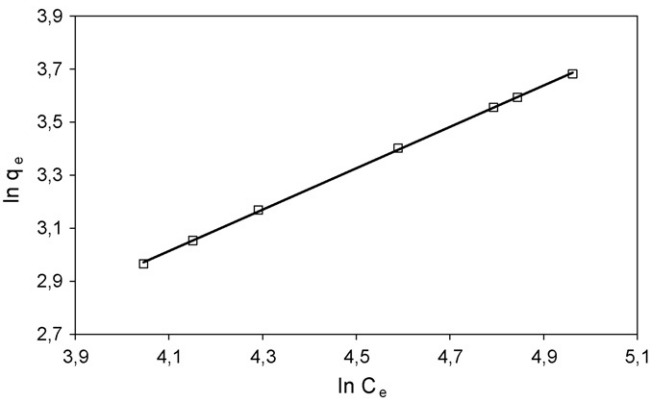

Fig. 6. Freundlich plot for copper removal by the ion exchange resin.

Table 3
Freundlich and Langmuir isotherm constants for copper removal by the ion exchange resin

Freundlich			Langmuir			
K_F ($mg^{1-(1/n)}\,L^{1/n}\,g^{-1}$)	n	R	q_m ($mg\,g^{-1}$)	b ($L\,mg^{-1}$)	R	R_L
0.829	1.281	0.999	121.50	3.365×10^{-3}	0.999	0.598

The Langmuir model makes several assumptions, such as monolayer coverage and constant adsorption energy while the Freundlich equation deals with heterogeneous surface adsorption. The applicability of both Langmuir and Freundlich isotherms to the studied system implies that both monolayer adsorption and heterogeneous surface conditions exist under the used experimental conditions. This finding is similar to that made in previous works on copper removal by ion exchange resins [5,26,27].

These experimental data are generally used in further studies concerning the dynamic exchange of solute in column studies for the prediction of breakthrough curves. However, it is important to note that exchange isotherms and constants determined in a fixed bed should be used for evaluating the breakthrough curves and kinetic constants to model such a system mathematically.

4.5. Breakthrough curves for copper removal

Most ion exchange operations are carried out in fixed beds of resin contained in vertical cylindrical columns. Batch equilibrium and kinetic tests are often complemented by dynamic column studies to determine system size requirements, contact time, and ion exchange resin usage rates. These parameters can be obtained from the breakthrough curves. Fixed bed ion exchangers share a common theory with fixed bed adsorbers.

The exchange breakthrough curves obtained by varying the bed height from 8 to 16 mm for different flow rates (39, 55, and 106 $mL\,h^{-1}$) and 200 $mg\,L^{-1}$ initial copper concentration for ion exchange resin are given in Fig. 7. The breakthrough curves are obtained by plotting the variation of solute concentration in the aqueous solution with time. Fig. 7 shows that for short times copper cations in the feed are taken up completely by the column. After a while metal breakthrough occurs and the effluent concentration increases with time. The saturation point is reached when the effluent concentration becomes equal to the feed concentration.

The variation of breakthrough and saturation times with respect to operating variables, influent flow rate and bed height is shown in Fig. 7. It was shown that breakthrough generally occurred faster with higher flow rate. Increases in both the breakpoint and saturation time with decreasing flow rate were observed. This behavior can be explained in terms of residence time of the metal in the column. When at a low rate of influent, copper had more time to contact with resin beads that resulted in higher removal of copper ions in column. The variation in the loading capacity may be explained on the basis of mass transfer fundamentals. The reason is that at higher flow rate the rate of mass transfer gets increases. The amount of copper exchanged with unit bed height (mass-transfer zone) increased with increasing flow rate leading to faster saturation at higher flow rate. At the highest flow rate, the lowest copper removal efficiency was observed. This behavior can be due to the insufficient contact time between the metal ions and the cation exchange resin, which limits the number of available active sites, thus reducing the volume of copper solution to be treated.

As the height of the bed decreases, the times required to reach the breakthrough and saturation points decreased. The mass of the

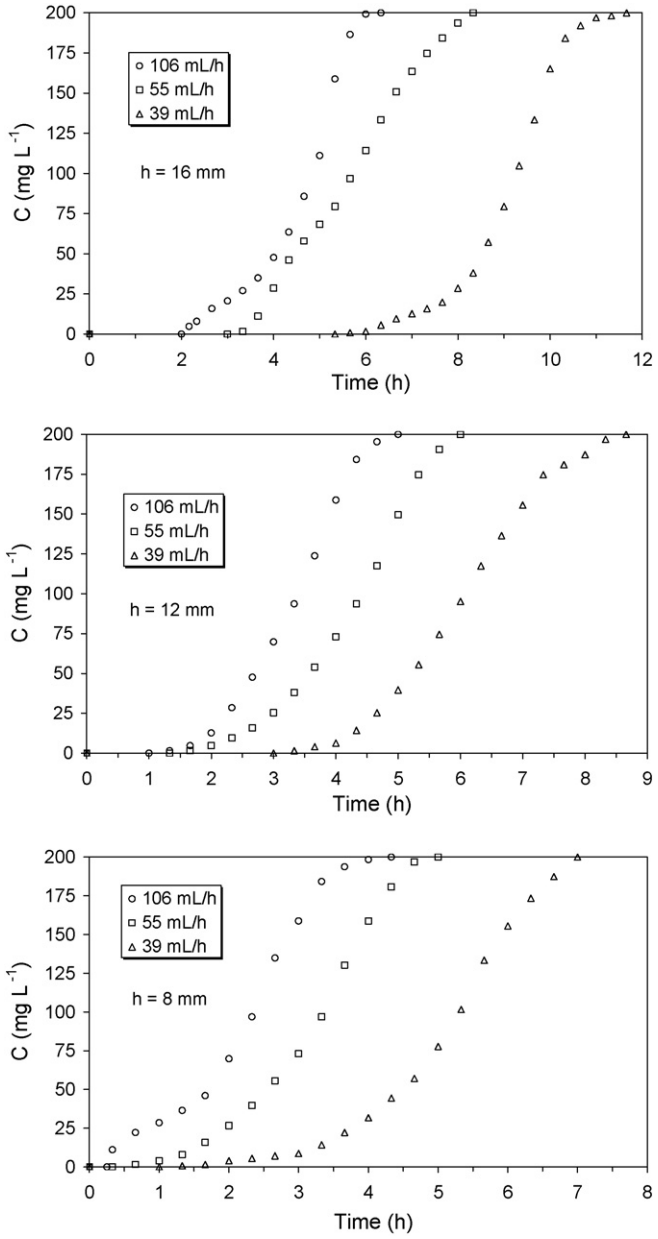

Fig. 7. Breakthrough curves for the removal of copper by the ion exchange resin at different bed heights and flow rates.

resin forming the fixed bed is proportional to the bed height and as a result the number of functional groups increases with the increase in bed height leading to a larger exchange capacity and delaying the occurrence of both breakthrough and saturation points. This means that the volume of copper solution that can be treated is effectively increased.

The comparative study of the effect of the operating conditions on resin exchange performance showed that both the breakthrough and saturation times depended on $1/U_0(1/Q)$ and Z parameters.

4.6. Modeling of breakthrough curves

Successful design of a column exchange process required prediction of the breakthrough curve for the effluent. Various mathematical models can be used to fit the exchange of copper in fixed bed columns. The dynamic behavior of the column is predicted with the Bohart–Adams, Bed Depth Service Time (BDST),

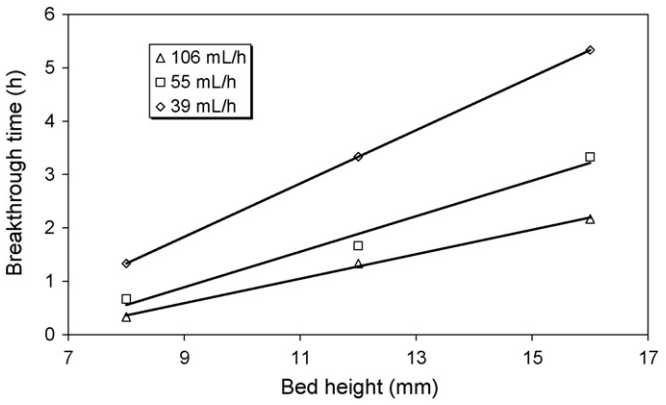

Fig. 8. BDST model plots for copper removal by the ion exchange resin at different flow rates.

Clark, and Wolborska models. The breakthrough curves showed the superposition of experimental results (points) and the theoretical calculated points (lines). Linear correlation coefficients (R) showed the fit between experimental data and linearized forms of the used equations while the average percentage errors (APE) calculated according to Eq. (16) indicated the fit between the experimental and predicted values of liquid-phase concentration used for plotting breakthrough curves.

$$\mathrm{APE}\,(\%) = \frac{\sum_{i=1}^{N} |(C_{\mathrm{experimental}} - C_{\mathrm{predicted}})/C_{\mathrm{experimental}}|}{N} \times 100 \quad (19)$$

where N the number of experimental data.

4.6.1. Application of the Bohart–Adams model

The calculation of theoretical breakthrough curves for a single-component system requires the determination of the parameters K_{BA} and N_0 for the solute of interest. These values may be determined from available experimental data. The approach involves a plot of $\ln[(C/C_0)-1]$ versus time according to Eq. (2).

The model developed by Bohart and Adams is applied to investigate the breakthrough behavior of copper by the ion exchange resin. The values of K_{BA} (the kinetic constant) and N_0 (the maximum amount of metal exchanged) are determined from $\ln[(C/C_0)-1]$ against t plots at different flow rates varied between 39 and 106 mL h^{-1} and at different bed heights varied between 8 and 16 mm. These values are used to calculate the breakthrough curve. The values of K_{BA} and N_0 are also listed in Table 4. The values of kinetic constant was influenced by flow rate and increased with increasing flow rate. However, for the higher flow rate (106 mL h^{-1}), the maximum amount of metal exchanged showed a larger deviation from the theoretical value compared with that calculated using the BDST model whatever the bed height.

The theoretical curves are compared with the corresponding experimental data in Fig. 9 and the obtained average percentage error values are regrouped in Table 4. The experimental breakthrough curves are very close to those predicted by the Bohart–Adams model. Thus, from the experimental results and data regression, the Bohart–Adams model provided a good correlation of the effects of bed height and flow rate.

4.6.2. Application of the bed depth service time (BDST) model

According to Eq. (3), the breakthrough time depends on $1/C_0$, $1/U_0$, and Z parameters, as shown by previous experimental results. The plot of breakthrough time against bed height at various flow rates for the present system is shown in Fig. 8. The high value of correlation coefficient ($R \geq 0.99$), confirms the good fit of this model and infers that the BDST model was successful in describing the

Table 4
Bohart–Adams model parameters for copper removal by the ion exchange resin at different bed heights and flow rates

Z (mm)	Q (mL h^{-1})	K_{BA} (L mg^{-1} h^{-1}) × 10^3	N_0 (mg L^{-1})	n_0 (mg g^{-1})	$-R$	APE (%)
16	106	9.29	113317.35	141.65	0.934	27.27
	55	6.88	78725.37	98.41	0.968	10.93
	39	8.23	86806.87	108.51	0.987	12.3
12	106	11.61	114349.3	142.94	0.992	12.3
	55	8.61	77539.03	96.92	0.992	13.17
	39	7.95	78960.27	98.7	0.994	11
8	106	9.65	107488.47	134.36	0.974	18.46
	55	9.59	85182.93	106.48	0.985	13.03
	39	6.99	99731.28	124.66	0.994	12.1

Table 5
BDST model parameters for copper removal by the ion exchange resin at various flow rates

Q (mL h^{-1})	Z_0 (mm)	N_0 (mg L^{-1})	n_0 (mg g^{-1})	R
106	6.42	96264	120.33	0.999
55	6.33	73238	91.55	0.99
39	5.33	77938	97.42	1

breakthrough for the removal of copper by the cation exchange resin. Parameters of the BDST equation are shown in Table 5. The maximum amount of metal exchanged and reaction zone values are strongly dependent on the flow rate. One might assume that the exchange process is significantly influenced by the external mass transfer of the solute through the hydrodynamic boundary layer. A higher value of the amount of copper exchanged was obtained as the bed height was increased, indicating that higher bed depth may be required for copper removal. The fixed bed exchange capacity obtained for a bed height of 16 mm is very close to the value determined in the batch process. The thickness of mass-transfer zone increases with the flow rate showing the widening of the reaction zone and appearance of a faster breakthrough. However, it can be supposed that minimum bed length would be short at the lowest flow rate. Under these experimental conditions, results suggest that the resin columns performance is characterized by a low critical bed length which increases with the column flow rate.

4.6.3. Application of the Clark model

In the batch equilibrium study, it was found that the Freundlich model fit the removal of copper by the ion exchange resin. Therefore, the Freundlich constant n was used to calculate the parameters in the Clark model. From a plot of $\ln[(C_0/C)^{n-1} - 1]$ versus time, the values of r (h^{-1}) and A can be thus determined from its slope and intercept, respectively. The parameters of the Clark equation and the correlation coefficients (R) for all flow rates and bed heights are given in Table 6. The correlation coefficients for the linear regression are acceptable showing good agreement of Clark model with the experimental data.

Table 6
Clark model parameters for copper removal by the ion exchange resin at different bed heights and flow rates

Z (mm)	Q (mL h^{-1})	ln A	r (h^{-1})	$-R$	APE (%)
16	106	4.31	1.42	0.877	45.55
	55	4.09	1.02	0.983	10.39
	39	8.65	1.19	0.956	27.42
12	106	3.56	1.65	0.975	19.42
	55	3.22	1.17	0.973	20.95
	39	5.16	1.15	0.985	13.4
8	106	1.46	1.58	0.948	30.08
	55	2.37	1.35	0.951	26.93
	39	2.82	0.89	0.97	33.26

The breakthrough curves predicted by the Clark model are shown in Fig. 9. It is clear from the figure and average percentage

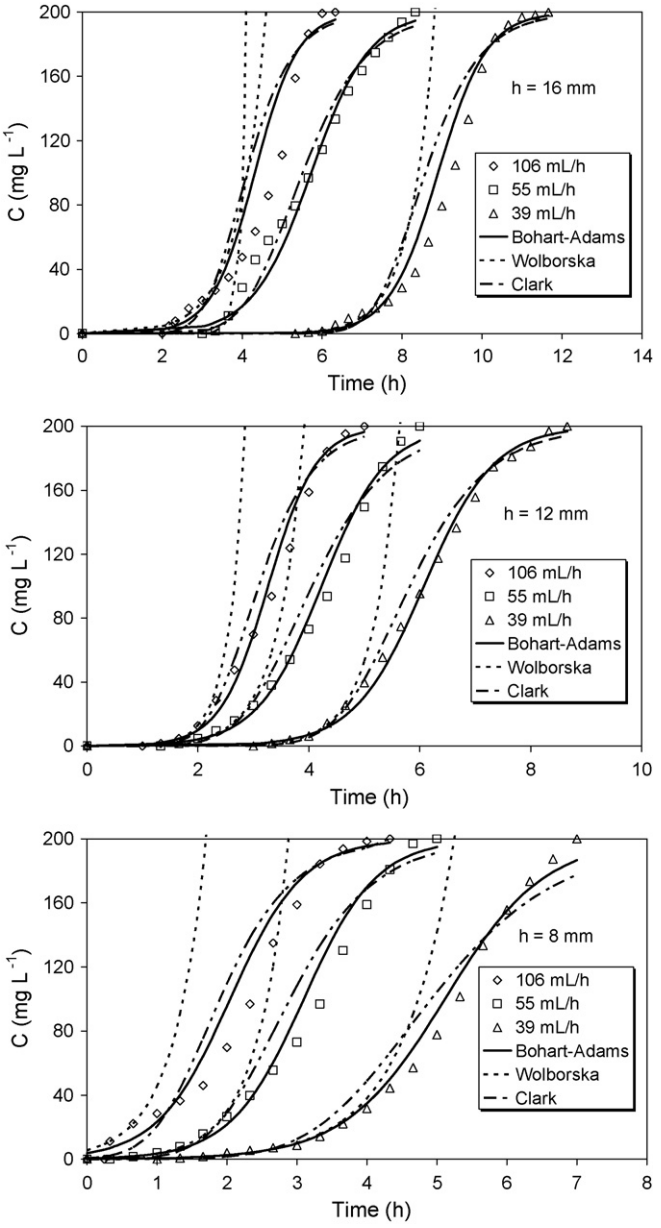

Fig. 9. Comparison of the experimental and theoretical breakthrough curves obtained at different flow rates and bed heights according to the studied models for copper removal by the cation exchange resin.

Table 7
Wolborska model parameters for copper removal by the ion exchange resin at different bed heights and flow rates

Z (mm)	Q (mL h^{-1})	β_a (h^{-1})	N_0 (mg L^{-1})	n_0 (mg g^{-1})	v (mm h^{-1})	R	APE (%)
16	106	870.62	121070.78	151.34	3.46	1	14.65
	55	1682.04	57065.7	71.33	3.84	1	0.05
	39	696.59	86142.34	107.68	1.81	0.95	33.15
12	106	1563.87	100826.54	126.03	4.16	0.999	3.29
	55	728.95	72130.42	90.16	3.04	0.983	16.24
	39	752.05	73399.38	97.75	2.12	0.996	8.26
8	106	940.83	89526.12	111.91	4.68	1	0
	55	839.49	79765.31	99.71	2.75	0.995	8.9
	39	676.62	102557.03	128.2	1.52	0.976	20.23

errors shown in Table 7 that the model fit reasonably the experimental results. It seems that the Clark parameter r decreases with the decrease of flow rate.

From the experimental results and data regression, the Clark model provided an acceptable correlation of the effects of bed height and flow rate.

4.6.4. Application of the Wolborska model

Analysis of exchange-column performance has been attempted by means of the Wolborska model that is used for the description of breakthrough curve in the range of the low-concentration. According to the Wolborska model, the breakthrough curves were linearized by plotting $\ln C/C_0$ versus t to determine the column parameters, the maximum amount of metal exchanged (N_0) and kinetic coefficient of the external mass transfer (β_a). A linear relationship between $\ln C/C_0$ and t is obtained for $\ln C/C_0 < -2$, for all breakthrough curves ($R \geq 0.95$). The values of the Wolborska model parameters at all flow rates and bed heights studied are presented in Table 7 together with the correlation coefficients. The migration velocity, v, was calculated by the Wolborska method and the values are set between 1.52 and 4.68 mm h^{-1} and increases with increasing the flow rate. The mass-transfer coefficient, β_a, is an effective coefficient which reflects the effect of both mass transfer in liquid phase and axial dispersion. Wolborska observed that in short beds or at high flow rates of solution through the bed, the axial diffusion is negligible and $\beta_a = \beta_0$, the external mass-transfer coefficient. Increasing flow rate from 39 to 106 mL h^{-1} increased the β_a value since increased turbulence reduces the film boundary layer surrounding the sorbent particle. On the other hand, the maximum amount of metal exchanged determined by this method showed, in four cases, a larger deviation from the theoretical value compared with that calculated using the BDST model.

Predicted and experimental breakthrough curves with respect to flow rate and bed height are shown in Fig. 9. It is clear from Fig. 9 and average percentage errors (11.64%) in Table 7 that there is a good agreement between the experimental and predicted values, suggesting that the Wolbraska model is valid for the concentration region up to 20 mg L^{-1} whereas large discrepancies are found between the experimental and predicted curves above this level for the copper removal by the ion exchange resin in fixed bed column.

5. Conclusions

The removal of copper(II) from aqueous solution of 200 mg L^{-1} initial concentration by the cation exchange resin-packed columns was investigated.

The equilibrium distribution of copper ions between resin and liquid phases was modeled by the Langmuir and the Freundlich isotherm equations. It was found that equilibrium data can be fitted by the both models.

The uptake of Cu(II) by the resin follows first-order kinetics. The influence of stirring speed and temperature on the removal kinetics was studied. When the stirring speed is higher than 110 rpm, the apparent rate constant is independent of stirring speed. The process is controlled by chemical rate as the diffusion in the resin particles is not the limiting step for a temperature of 25 °C. The liquid-film diffusion is the limiting step and controls the exchange process when the stirring speed is lower than 110 rpm. The plot of $\ln K_{app} = f(1/T)$ shows two linear regions. The initial linear portion obtained at low temperatures ($T < 45$ °C) corresponds to the kinetic mode and the activation energy for the exchange reaction was determined (13.58 kJ mol^{-1}). The linear portion obtained for high temperatures (>45 °C) is attributed to the transport phenomena inside solid pellets.

The breakthrough curves have been determined at various flow rates and bed heights at 25 °C. The obtained results showed that both breakthrough and exhaustion times increase with the increase in the height of the bed, as more binding sites are available. For a given bed height, the higher the flow rate is, the lower are the breakthrough and exhaustion times. This flow rate dependence can be accounted for by the fact that for lower value of flow rate, the contact time is longer and hence the interaction between the metal and the resin is also greater.

Several models were applied to experimental data obtained from dynamic studies performed on fixed columns to predict the breakthrough curves and to determine the column kinetic parameters. These models gave good approximations of experimental behavior. The simulation of the whole breakthrough curve is effective with the Bohart–Adams and the Clark models, but the Bohart–Adams model is better. The breakthrough data gave a good fit to the BDST model, resulting in a bed exchange capacity very close to the value determined in the batch process. A linear relationship between $\ln(C/C_0)$ and time at a given bed height and flow rate was obtained with all breakthrough curves in the region up to 20 mg L^{-1}, suggesting that the initial segment of the breakthrough curve fit the Wolborska model, and allowing the kinetic coefficients of mass transfer in the fixed bed to be estimated.

Acknowledgements

This work was financially supported by the Ministry of Higher Education and Scientific Research of Algeria (Project No. J 0101120060043). The author thanks Mrs. L. Senani and Mr. F. Balaska for their helpful cooperation in the experimental tests.

References

[1] J.W. Patterson, Metal Speciation Separation and Recovery, Lewis Publishers, Chelsea, MI, 1987.
[2] J. Yang, A. Renken, Heavy metal adsorption to a chelating resin in a binary solid fluidized bed, Chem. Eng. Technol. 23 (2000) 1007–1012.

[3] K.S. Rao, D. Sarangi, P.K. Dash, G.R. Chaudhury, Treatment of wastewater containing copper, zinc, nickel and cobalt using Duolite ES-467, J. Chem. Technol. Biotechnol. 77 (2002) 1107–1113.
[4] F. Gode, E. Pehlivan, A comparative study of two chelating exchange resins for the removal of chromium(III) from aqueous solution, J. Hazard. Mater. B100 (2003) 231–243.
[5] S.H. Lin, C.D. Kiang, Chromic acid recovery from waste acid solution by an ion exchange process: equilibrium and column ion exchange modelling, Chem. Eng. J. 92 (2003) 193–199.
[6] A. Dabrowski, Z. Hubicki, P. Podkoscielny, E. Robens, Selective removal of heavy metal ions from waters and industrial wastewaters by ion-exchange method, Chemosphere 56 (2004) 91–106.
[7] S. Rengaraj, S.H. Moon, Kinetics of adsorption of Co(II) removal from water and wastewater by ion exchange resins, Water Res. 36 (2002) 1783–1793.
[8] M.E. Malla, M.B. Alvarez, D.A. Batistoni, Evaluation of sorption and desorption characteristics of cadmium, lead and zinc on Amberlite IRC-718 iminodiacetic chelating ion exchanger, Talanta 57 (2002) 277–287.
[9] R.K. Sharma, N. Bhojak, S. Mittal, B.S. Garg, Chelating resins and their applications in the analysis of trace metal ions, Microchem. J. 61 (1999) 94–114.
[10] J. Lehto, A. Paajanen, R. Harjula, H. Leinonen, Hydrolysis, H^+/Na^+ exchange by Chelex 100 chelating resin, React. Polym. 23 (1994) 135–140.
[11] L.C. Lin, R.S. Juang, Ion-exchange equilibria of Cu(II) and Zn(II) from aqueous solutions with Chelex 100 and Amberlite IRC 748 resins, Chem. Eng. J. 112 (2005) 211–218.
[12] M.G. Rao, A.K. Gupta, E.S. Williams, A.A. Aguwa, Sorption of heavy metal ions on Chelex 100 resin, AIChE Symp. Ser. 78 (219) (1982) 103–111.
[13] C.N. Haas, V. Tare, Application of ion exchangers to recovery of metals from semiconductor wastes, React. Polym. 2 (1984) 61–70.
[14] V. Tare, S.B. Karra, C.N. Haas, Kinetics of metal removal by chelating resin from a complex synthetic wastewater, Water, Air, Soil Pollut. 22 (1984) 429–439.
[15] E. Korngold, N. Belayev, L. Aronov, S. Titelman, Influence of complexing agents on removal of metals from water by a cation exchanger, Desalination 133 (2001) 83–88.
[16] T.H. Karppinen, A.Y. Pentti, Evaluation of selective ion exchange for nickel and cadmium uptake from the rinse water of a plating shop, Sep. Sci. Technol. 35 (2000) 1619–1633.
[17] F. Gode, E. Pehlivan, A comparative study of two chelating exchange resins for the removal of chromium(III) from aqueous solution, J. Hazard. Mater. B 100 (2003) 231–243.
[18] F. Mijangos, M. Diaz, Metal–proton equilibrium relations in a chelating iminodiacetic resin, Ind. Chem. Eng. Res. 31 (1992) 2524–2532.
[19] A. Sahel, Contribution à l'étude en régime dynamique de la sorption sur charbon actif de molécules organiques. Comparaison et simplification de différents modèles, Ph.D. Thesis, University of Limoges, No. 4, 1993.
[20] G. Bohart, E.N. Adams, Some aspects of the behavior of charcoal with respect to chlorine, J. Am. Chem. Soc. 42 (1920) 523–544.
[21] R.A. Hutchins, New method simplifies design of activated carbon systems, Chem. Eng. 80 (1973) 133–135.
[22] R.M. Clark, Evaluating the cost and performance of field-scale granular activated carbon systems, Environ. Sci. Technol. 21 (1987) 573–580.
[23] A. Wolborska, Adsorption on activated carbon of *p*-nitrophenol from aqueous solution, Water Res. 23 (1989) 85–91.
[24] I. Rodríguez Iznaga, V. Petranovskii, G. Rodríguez Fuentes, C. Mendoza, A. Benítez Aguilar, Exchange and reduction of Cu^{2+} ions in clinoptilolite, J. Colloid Interface Sci. 316 (2007) 877–886.
[25] N.F. Chelishchev, B.F. Volodin, B.L. Kriukov, Ionic Exchange in High-silica Natural Zeolites, Nauka, Moscow, 1988, p. 32.
[26] A. Demirbas, E. Pehlivan, F. Gode, T. Altun, G. Arslan, Adsorption of Cu(II), Zn(II), Ni(II), Pb(II), and Cd(II) from aqueous solution on Amberlite IR-120 synthetic resin, J. Colloid Interface Sci. 282 (2005) 20–25.
[27] S. Rengaraj, J.-W. Yeon, Y. Kim, Y. Jung, Y.-K. Haa, W.-H. Kima, Adsorption characteristics of Cu(II) onto ion exchange resins 252H and 1500H: kinetics, isotherms and error analysis, J. Hazard. Mater. B 143 (2007) 469–477.
[28] K.R. Hall, L.C. Eagleton, A. Acrivos, T. Vermeulen, Pore and solid diffusion kinetics in fixed bed adsorption under constant pattern conditions, Ind. Eng. Chem. Fundam. 5 (1966) 212–223.
[29] R.E. Treybal, Mass-transfer operations, 3rd edn., McGraw Hill, 1980.